Ocean Engineering 106 (2015) 281–288

Contents lists available at ScienceDirect

Ocean Engineering

journal homepage: www.elsevier.com/locate/oceaneng

Numerical modelling of rotor–stator interaction in rim driven thrusters

Aleksander J. Dubas [a,b,*], N.W. Bressloff [b], S.M. Sharkh [b]

[a] Institute of Complex Systems Simulation, University of Southampton, UK
[b] Faculty of Engineering and Environment, University of Southampton, UK

ARTICLE INFO

Article history:
Received 27 January 2014
Accepted 9 July 2015

Keywords:
Frozen rotor
Unsteady
Numerical
CFD
Thruster
Rim driven

ABSTRACT

An electric rim driven thruster is a relatively new marine propulsion device and the associated fluid dynamics have not been fully investigated. This work develops a robust CFD method and investigates both frozen rotor and unsteady simulations of rotor–stator interaction. Two solvers from OpenFOAM were used. Steady state simulations were performed using MRFSimpleFoam with a frozen rotor treatment of the interface between static and rotational reference frames. The solver for unsteady simulations was pimpleDyMFoam, utilising a sliding mesh interface to handle the dynamic meshing. Both methods are thoroughly verified and validated against experimental data. The *k*–omega SST turbulence model is found to be robust down to low advance ratios. For the rim driven thruster, analytical models are used to estimate friction forces in the rim gap and their contribution to torque losses. The frozen rotor and unsteady treatments of rotor–stator interaction are compared and found to have similar trends in the variation of thrust produced. However, the frozen rotor method does not predict the same variation of instantaneous torque and does not capture the rotor–stator interaction fully. Analysis of the unsteady rotor–stator interaction shows an oscillating flow over the stators and thus inflow to the blades.

1. Introduction

An electric rim driven thruster is a relatively new marine propulsion device which uses a permanent magnet rotor built into a rim around the propeller (Sharkh et al., 2003). In many ways, rim driven thrusters are hydrodynamically similar to ducted propellers but with a major difference: there is no propeller tip clearance or leakage losses. However, the penalty for this advantage is that there may be leakage around the rim and significant friction losses in the gap between the rim and the duct.

A simplified cross section of the rim driven thruster studied in this paper is shown in Fig. 1 with the key parts identified. Starting from the outside, there is a duct which also houses the static parts of the motor. Attached to the duct is a set of hydrodynamic stators which, as the device is bi-directional, serve as both pre-stators and post-stators depending on the direction of thrust. These stators are also a structural component that house and centre the hub and shaft bearings, thus inserted into the stator/hub assembly is the shaft. On the shaft the propeller blades are mounted, and at the blade tips a rim is included which also houses the rotating parts of the motor.

Rim driven thrusters are normally designed to be bi-directional as there is no need for an upstream shaft or gearbox, allowing for a symmetrical geometry and thus equal performance in both operational directions. Lea et al. (2003) investigated commercial rim driven thrusters experimentally and found that they had increased efficiency, flexibility and manoeuvrability compared to conventional propulsors. This was attributed to the torque response of the permanent magnet motors as well as better tip loading and cavitation performance due to the presence of the rim.

A number of different methods have been used previously to model the performance and flow field of rim driven thrusters, from boundary element methods to finite volume Reynolds-Averaged Navier Stokes (RANS) methods; the latter being the preferred method in recent literature. Kinnas et al. (2009) conducted a numerical prediction of performance and sheet cavitation of a rim driven tunnel thruster using combined RANS and boundary element methods. The boundary element method was used to calculate thruster performance, which was subsequently fed into a commercial RANS code as a body force to calculate the inflow to the propeller. The inflow profile was then fed iteratively back into the boundary element code until thrust and torque coefficient had converged. This method predicted thrust very well at high rotational speeds. At low speeds thrust was over-predicted, due to the boundary element method's inability to capture the off-design flow field correctly.

Yakovlev et al. (2011) used a pure RANS code for their modelling, correctly predicting performance over a larger operating range, and applied their code to a design optimisation study of the pitch distribution to produce a 0.4% increase in efficiency that was

* Corresponding author.
E-mail address: ajd205@soton.ac.uk (A.J. Dubas).

http://dx.doi.org/10.1016/j.oceaneng.2015.07.012
0029-8018/

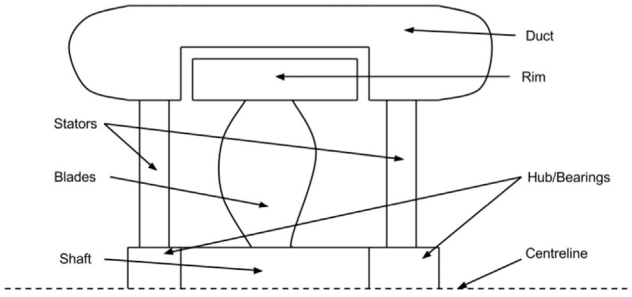

Fig. 1. Cross-section diagram of rim driven thruster.

subsequently experimentally verified. Additionally, the induced stresses in the blades in various configurations were investigated and it was found that there was a six-fold reduction of peak stress, which is another advantage of a rim drive. This allows designs to be produced with thinner, more hydrodynamically efficient, blades.

Cao et al. (2012) simulated a rim driven thruster using RANS, combined with analytical models to describe the torque production of the Taylor–Couette flow in the gap between the rim and the duct. This is a large source of losses in rim driven thrusters, contributing to 27% of the total torque in the work of Cao et al. (2012), although the simulation was simplified through the use of discrete analytical models for the torque. The rim drive thruster studied by Cao et al. (2012) differs from the present one by being both hubless and statorless.

In some cases stators have been shown to be beneficial to propulsive efficiency (Celik and Guner, 2007) and it may be possible to exploit the stators in a rim driven thruster. The rim driven thruster investigated in this paper utilises the stators primarily for locating the spindle and bearings, and they may be adapted to improve the hydrodynamic efficiency, but to preserve the bi-directional performance the stators must function as both pre-stators and post-stators.

It is possible to include the rotor–stator interaction either through use of multiple steady-state simulations using a frozen rotor formulation or through a more computationally expensive unsteady simulation. The authors are not aware of any previous work on unsteady modelling of rotor–stator interaction in rim driven thrusters. Petit et al. (2009) found that steady-state frozen rotor formulations are not sufficiently accurate for capturing the rotor–stator interaction in a centrifugal pump due to the improper treatment of the impeller wake. However, using a series of frozen rotor simulations at different relative displacements, Li and Wang (2007) modelled the rotor–stator interaction in an axial pump without explicit consideration of the unsteady effects and achieved good results.

The present work builds on previous work by the authors (Dubas et al., 2011), which investigated the steady-state simulation of a rim driven thruster with 70 mm propeller design and found that the use of steady-state simulations in the presence of stators caused a significant reduction in accuracy due to the poor modelling of the rotor–stator interaction. A similar modelling method to that of Cao et al. (2012) is used in the present work, excluding the rim gap from the CFD and instead modelling its effects analytically, but this geometry also requires simulation of the rotor–stator interaction. To investigate improving the capture of rotor–stator interaction, this work uses two methods, one steady-state and one time-varying, and compares the effect of rotor–stator interaction between the two methods.

2. Methods

2.1. Meshing

The rim driven thruster used in this study is a 100 mm diameter bi-directional thruster, similar to the one pictured in Fig. 2. This device was selected due to the availability of experimental thrust and torque data. Import of the geometry into the meshing program was through the .stl file format from the SolidWorks geometry originally provided.

The mesh generation was subsequently performed using the blockMesh and snappyHexMesh applications within OpenFOAM. A base hexahedral mesh with an edge length of one-half of the propeller diameter was generated using blockMesh. The computational domain extents were also defined in the base mesh (see Fig. 3), with the final domain extending five propeller diameters upstream of the device, six diameters in the radial direction and 10 diameters downstream of the device; these dimensions were determined based on the verification procedure discussed in Section 2.2. The boundary conditions were set to a constant velocity inlet, with a symmetry plane in the radial directions, that is the positive and negative x and y Cartesian directions, and a constant pressure outlet. On the propeller surface, the mesh edge length was set to 1/256th of the propeller diameter, with no wall functions used as the average y_1^+ was four and for visual reference the meshed surface is shown in Fig. 4. For meshing of the open water propeller, the rotating reference frame region had a radius of 1.14 times the propeller radius, extending past the propeller tips. It has been shown that the size of this region needs to be sufficiently large and is critical to accuracy when using Multiple Reference Frame (MRF) methods for open water propellers (Kaufmann and

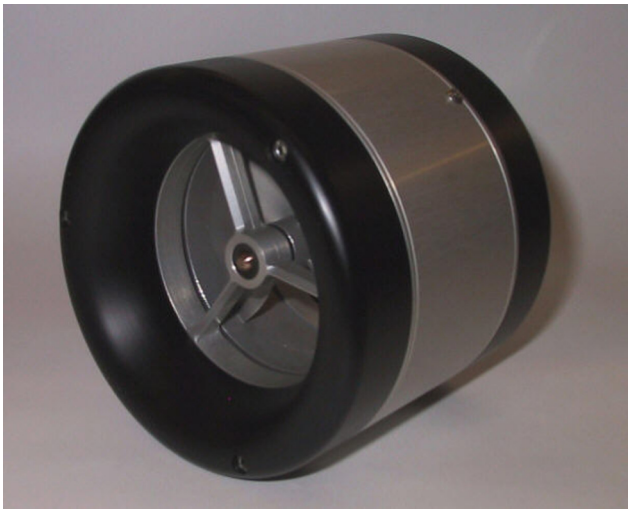

Fig. 2. Integrated Thruster by TSL Technology Ltd.

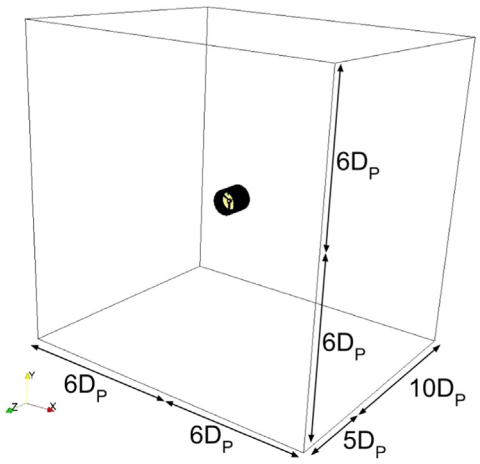

Fig. 3. Rim driven thruster meshed domain showing distances to boundaries where D_P is the propeller diameter.